

A structural test for the conformal invariance of the critical 3d Ising model

Simão Meneses¹, Slava Rychkov^{2,3,4}, J. M. Viana Parente Lopes¹, Pierre Yvernay⁴

¹ *Centro de Física das Universidades do Minho e Porto Departamento de Engenharia Física, Faculdade de Engenharia and Departamento de Física e Astronomia, Faculdade de Ciências, Universidade do Porto, 4169-007 Porto, Portugal*

² *Institut des Hautes Études Scientifiques, Bures-sur-Yvette, France*

³ *Laboratoire de physique théorique, Département de physique de l'ENS, École normale supérieure, PSL University, Sorbonne Universités, UPMC Univ. Paris 06, CNRS, 75005 Paris, France*

⁴ *Theoretical Physics Department, CERN, Geneva, Switzerland*

How can a renormalization group fixed point be scale invariant without being conformal? Polchinski (1988) showed that this may happen if the theory contains a virial current – a non-conserved vector operator of dimension exactly $(d - 1)$, whose divergence expresses the trace of the stress tensor. We point out that this scenario can be probed via lattice Monte Carlo simulations, using the critical 3d Ising model as an example. We measure the scaling dimension of the lowest virial current candidate V , and find $\Delta_V = 6 \pm 1$, well above 2 expected for the true virial current. Our result shows that the critical 3d Ising model has no virial current, providing a structural explanation for the conformal invariance of the model.

Dedicated to the memory of Joe Polchinski

Contents

1. Introduction	1
2. Lattice setup	3
2.1. Choice of Monte Carlo algorithm	5
3. Results	6
4. Conclusions	8
A. Dimension of V in the ϵ expansion	11
B. Comment on Ref. [10]	11
C. Possible boundary conditions	13
C.1. Gluing b.c.	13
C.2. Changing the strength of boundary interactions	13
D. Heuristic optimization of boundary conditions	14

1. Introduction

It is believed that the critical point of the 3d ferromagnetic Ising model is conformally invariant. One strong piece of evidence is the excellent agreement between the critical exponents extracted from the experiments and Monte Carlo simulations and from the conformal bootstrap [1,2]. Conformal invariance has been also checked directly on the lattice, by verifying functional constraints that it imposes on the shape of some correlation function observables [3].¹ The main purpose of our paper is to provide another lattice test of this property, which is qualitatively different and in a sense more robust.

Any field theory coming from a local action, and in particular the 3d Ising model close to or at the critical temperature, has a local stress tensor operator $T_{\mu\nu}$ which is conserved: $\partial^\mu T_{\mu\nu} = 0$. The structural property of *conformally invariant* local theories is that this local stress tensor operator is traceless:

$$T_\mu{}^\mu = 0. \tag{1.1}$$

Our new test will probe this structural property of conformal invariance, unlike previous lattice studies which tested its consequences.

¹We would also like to point out a related lattice study of conformal invariance in 3d percolation [4].

The key question is: could the critical 3d Ising model be scale invariant (as befits any critical theory, being a fixed point of a renormalization group flow), but not fully conformally invariant? As was lucidly explained by Polchinski [5],² a theory will be scale invariant without being conformal if $T_{\mu\nu}$ is not traceless but rather is a total divergence:

$$T_{\mu}{}^{\mu} = \partial^{\nu} W_{\nu}, \quad (1.2)$$

where W_{μ} is a vector operator, called the virial current, which is (a) not conserved and (b) not itself a total derivative.³ Precisely this mechanism is responsible for scale without conformal invariance of the theory of elasticity, perhaps the simplest physically relevant example of this phenomenon [8].⁴

It's then natural to inquire if Eq. (1.2) can hold in the critical 3d Ising model, and we will show that it cannot. Our argument is based on the following simple observation: any operator W_{μ} which is a candidate to appear in the r.h.s. of (1.2) must have two additional properties. First of all, it should, just as $T_{\mu\nu}$ itself, be invariant under the internal symmetry of the model, \mathbb{Z}_2 in the case of Ising. In addition, since $T_{\mu\nu}$ has canonical scaling dimension d , operator W_{μ} should have dimension $d - 1 = 2$. We will show that there is no operator with such properties, and so (1.2) cannot hold.

Concretely, we will use lattice Monte Carlo simulations to measure the scaling dimension of the *lowest* \mathbb{Z}_2 -even vector operator V_{μ} in the critical 3d Ising model, which is not a total derivative. Our main result is

$$\Delta_V = 6 \pm 1. \quad (1.3)$$

In particular, since $\Delta_V > 2$, this proves that the 3d Ising model has no candidates for W_{μ} . This rules out the scale without conformal invariance scenario based on (1.2), and thus provides a new test of conformal invariance.⁵

Extending the discussion from $d = 3$ to the whole family of \mathbb{Z}_2 -invariant Wilson-Fisher fixed points for $2 \leq d \leq 4$, the dimension of V can be determined exactly in $d = 2$ and for d near 4. In the 2d Ising model, it is the Virasoro descendent of the Identity $V \sim L_{-2} \bar{L}_{-3} \mathbb{1}$ and has dimension 5. In $d = 4$ where the Wilson-Fisher fixed point becomes free, we have $V \sim \phi \partial_{\mu} \phi (\partial \phi)^2$ of dimension 7. In $4 - \epsilon$ expansion, the dimension of V is given by (see appendix A)

$$\Delta_V = 7 - (5/9)\epsilon + O(\epsilon^2). \quad (1.4)$$

²See also [6] for a review. Concerning the 3d Ising model, see especially section 4.2 of [7].

³If W_{μ} is a total derivative, the stress tensor can be “improved” to be traceless, so that Eq. (1.1) is satisfied for the improved $T_{\mu\nu}$.

⁴It should be noted that this mechanism may be realized with a quirk in gauge theories. Namely it may happen that Eq. (1.2) holds but that the virial current is not a gauge invariant operator (and so is not a physical local operator). For example, this is how the 3d Maxwell theory avoids conformal invariance [9].

⁵Delamotte, Tissier and Wschebor [10] claimed to have proven rigorously that $\Delta_V > 2$ in the 3d Ising model. In our opinion, their argument is flawed, see appendix B.

Based on these limiting cases, it is reasonable to expect that V in $d = 3$ has dimension between 5 and 7, and our result (1.3) conforms nicely with this expectation.

2. Lattice setup

We simulate the nearest-neighbor ferromagnetic 3d Ising model on the cubic lattice at the critical temperature. The Hamiltonian is

$$H = -\beta \sum_{\langle xy \rangle} s(x)s(y), \quad s(x) = \pm 1.$$

We use the known critical temperature $\beta = \beta_c \approx 0.2216546$ [11,12].

Our lattice has spatial extent $L \times L \times L$ sites. We set lattice spacing $a = 1$. Due to the difficulties of measuring a rather high scaling dimension Δ_V , we will only be able to go up to volumes $L = 16$. We impose periodic boundary conditions in directions x_1, x_2 , while at $x_3 = 0, L-1$ we impose a mixture of fixed and free boundary conditions. Namely, for $x_3 = 0$ we impose the fixed $s = +1$ boundary condition for points with $L/4 \leq x_1 < 3L/4$, while at $x_3 = L-1$ we do the same for points with $L/2 \leq x_1 < L$. The rest of the boundaries at $x_3 = 0, L-1$ has free boundary conditions (see Fig. 1). The reasons for such a bizarre choice of boundary conditions at $x_3 = 0, L-1$ will be explained shortly.

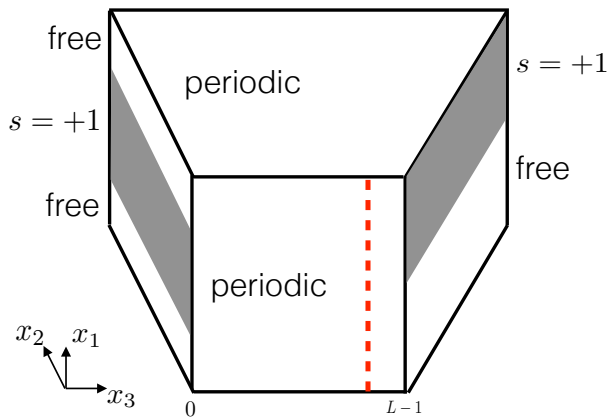


Fig. 1: The boundary conditions used in our simulation. The $x_3 = 0$ and $x_3 = L-1$ faces have a combination of free (white) and fixed $s = +1$ (gray) boundary conditions. On the other faces the periodic boundary conditions are imposed. This drawing uses the Byzantine perspective only to improve visibility; the actual geometry is an $L \times L \times L$ cube with parallel sides. The red dashed line is one possible location of the integrated observable (2.3).

We work with the lattice operator

$$V_\mu^{\text{lat}} = s(x) \nabla_\mu s(x) \sum_{\nu=1}^3 [\nabla_\nu s(x)]^2, \quad (2.1)$$

where x is a lattice point and

$$\nabla_\nu s(x) = s(x + \hat{e}_\nu) - s(x - \hat{e}_\nu)$$

is the symmetric lattice derivative in the ν direction.

Close to the critical point, the lattice operator V_μ^{lat} can be expanded into a basis of local operators of well-defined scaling dimensions. Since V_μ^{lat} is not a total derivative, the operator V_μ we are interested in will appear in this expansion:

$$V_\mu^{\text{lat}} = CV_\mu + \dots \quad (2.2)$$

The constant C is an unknown, non-universal, lattice quantity, and we will assume $C \neq 0$ since there is no reason to expect otherwise. The \dots includes various terms which we are not interested in, and we should make sure that those terms do not mask the contribution of V_μ . Some of these terms involve operators of higher scaling dimension than V . The presence of those terms is harmless since their effect will be subleading in the large volume limit. More annoying are the total derivative terms involving derivatives of various \mathbb{Z}_2 -even scalar operators which exist in the 3d Ising model (see Table 2 in [2]). Some of these have a rather low dimension and would mask V_μ unless special care is taken. For example, we expect $\partial_\mu \varepsilon$ to appear in the r.h.s. of (2.2), where ε is the lowest-dimension \mathbb{Z}_2 -even scalar, of dimension $\Delta_\varepsilon \approx 1.41$.

In our study we filter out the total derivative contributions through the following trick, rendered possible by the periodic boundary conditions. We consider the average value of the x_1 -component of V_μ^{lat} integrated along a periodic circle in this direction:

$$I(x_2, x_3) = \frac{1}{L} \sum_{x_1=0}^{L-1} V_1^{\text{lat}}(x_1, x_2, x_3) \quad (2.3)$$

Integration kills off the total derivative terms, so that this integrated observable couples in the continuum limit only to the integral of V_μ (plus the harmless higher-dimension non-derivative operators).

We will measure the dimension of V_μ by studying the one-point (1pt) function of I . In infinite volume vector operators would have zero 1pt functions, but in finite volume with appropriate boundary conditions they can be nonzero. In our case we will have

$$\langle I(x_2, x_3) \rangle \equiv \text{Obs}(x_3) = \frac{1}{L^{\Delta_V}} f\left(\frac{x_3}{L-1}\right) + \dots, \quad (2.4)$$

with no dependence on x_2 due to the translation invariance in that direction. The finite volume scaling is determined by the dimension of V , and this is how we will extract Δ_V .

Another way to determine Δ_V would be to impose periodic boundary conditions also in the x_3 direction and to study finite size scaling for the 2pt function of I at separation $L/2$. This observable would scale as $1/L^{2\Delta_V}$. We tried this strategy and found the signal completely swamped by noise, due to large Δ_V . Using the 1pt function improves the signal-to-noise ratio by a factor L^{Δ_V} and will allow us to perform the measurement.

The ... terms in (2.4) decay with a higher power of L . They originate from the higher-dimension operators contributing to V_μ^{lat} as well as from corrections to scaling arising from the fact that in finite volume the theory is not exactly at the critical point but is still flowing to it in the renormalization group sense. Because of limited statistics, we will unfortunately be forced to simply neglect both of these corrections in our analysis.

The function $f(t)$, $0 < t < 1$, parametrizes the observable (2.4) in the infinite-volume limit. This function will be measured in our simulation. To have nonzero $f(t)$, the boundary conditions at $x_3 = 0, L - 1$ should break the flip symmetry in the x_1 direction:

$$x_1 \rightarrow L - x_1,$$

under which I changes sign. This is the case for our boundary conditions in Fig. 1. On the other hand, our boundary condition preserves the above x_1 flip accompanied by the x_3 flip:

$$x_3 \rightarrow L - x_3,$$

and a periodic shift of the x_1 direction by $L/4$. As a consequence, our function $f(t)$ will be odd with respect to $t = 1/2$, and in particular $f(1/2) = 0$.

We have experimented with several other flip-breaking boundary conditions, and settled for the one in Fig. 1 because it gives rise to a particularly sizable $f(t)$, thus further improving signal-to-noise. See appendix C for a list of other possible boundary conditions, and appendix D for a heuristic procedure to quickly evaluate which boundary condition is expected to work best.

While it is not directly related to our computation, we would like to mention here one other instance where boundary conditions were used in lattice field theory to make a 1pt function of a tensor operator nonzero. Namely, in 4d lattice gauge theory, the 1pt function of the off-diagonal stress tensor component T_{0x} was measured imposing the “shifted” boundary conditions, when the fields are made periodic in the spatial directions, and periodic up to a coordinate shift in the Euclidean time direction [13]. This boundary condition is a particular case of the gluing boundary condition discussed in appendix C.

2.1. Choice of Monte Carlo algorithm

We perform Monte Carlo simulations using the single-spin-flip Metropolis algorithm. The choice of Monte Carlo algorithms plays a crucial role in the efficiency of the simulations. It is well known that the Wolff algorithm [14] is more efficient than the Metropolis algorithm at the critical

temperature due to the scaling of the computational effort with the system size. However, even though the smaller critical slowdown exponent favors the Wolff algorithm for large systems, for small ones and for some statistical observables, the Metropolis algorithm may be more efficient. This is what happened in our case.

To be more concrete, the standard measure of the simulation efficiency is based on the product of the algorithm execution time (τ_{CPU}) and the integrated autocorrelation time (τ_c). One reason to prefer the Metropolis algorithm is that in our case it led to very small integrated autocorrelation time of the vector operator sampling (this time scale depends on the statistical observable we are trying to measure).

Another important factor for this choice was the role of the boundary conditions. The use of fixed boundary conditions requires the imposition of an acceptance probability to flip the clusters touching the boundary (see appendix C). On the other hand, if we replace the fixed b.c. by the $\beta_{\text{bdry}} = \infty$ conditions (see appendix D) each time a cluster touches the boundary the full boundary will be flipped with a clear increase of τ_{CPU} and without any gain in τ_c . These reasons led us to opt for the Metropolis algorithm. Our tests showed that for a system size of $L = 16$, the Metropolis algorithm was able to produce results with error bars comparable to the Wolff algorithm, being faster by a factor of 10.

3. Results

We performed Monte Carlo simulations in the setup described in the previous section, with $L = 8, 12, 16$. The nature of our boundary conditions, with the shift by $L/4$, requires to increase L in steps of 4.

Our simulations were organized as follows. To generate the next sufficiently decorrelated spin configuration we performed $N = L^3/4$ steps of the Metropolis algorithm on spins with randomly chosen positions. The measurement of the observable $\text{Obs}(x_3)$ in (2.4) was then performed (averaging over x_2). Since our lattice operator (2.1) has range 3, we only did the measurement for $1 \leq x_3 \leq L - 2$.

The total number of such decorrelated spin configurations that we generated was 2.4×10^{12} (resp. 3.5×10^{13}) for $L = 12$ (resp. $L = 16$). A much smaller number sufficed for $L = 8$. For $N = L^3/4$ spin flips between the two measurements, the integrated autocorrelation time between the subsequent measurements of $\text{Obs}(x_3)$ was close to 1 for every x_3 .

Our simulations were parallelized on a cluster and took a total of about 300 CPU-years.

The numerical results of these measurements are given in table 1, and are shown in plots below as a function of $t = x_3/(L - 1)$.⁶ In these plots we show the data multiplied by $(L/12)^\Delta$

⁶The raw data in text form can be found inside the tex file of the arxiv submission.

x_3	Obs(x_3) in units of 10^{-6}		
	$L = 8$	$L = 12$	$L = 16$
1	41.9(7)	9.33(17)	3.11(9)
2	12.5(7)	3.12(19)	1.08(9)
3	1.7(7)	0.87(19)	0.49(10)
4	-3.5(7)	0.74(20)	0.27(10)
5	-10.7(7)	-0.24(20)	0.12(10)
6	-41.7(7)	0.16(20)	-0.03(10)
7		-0.39(20)	0.06(10)
8		-1.02(19)	-0.13(10)
9		-3.18(19)	-0.08(10)
10		-9.07(17)	-0.07(10)
11			-0.25(10)
12			-0.51(10)
13			-1.07(10)
14			-3.13(10)

Table 1: Results of Monte Carlo measurements with statistical errors.

for various values of Δ . According to (2.4), the curves for different L are supposed to collapse if $\Delta = \Delta_V$. At least this is supposed to happen for sufficiently large L , when contributions from the subleading terms ... in (2.4) become unimportant.

In Fig. 2 we take $\Delta = 2$, the value needed for a virial current candidate. Clearly the curves show no collapse, ruling out the existence of the virial current.

A side remark: as mentioned in the previous section, the function $f(t)$ should be odd with respect to $t = 1/2$ for our choice of the boundary conditions. This antisymmetry is indeed satisfied within error bars, as can be seen in the figures.⁷

In Fig. 3 we show what the same plot looks like if we choose $\Delta = 6$. In fact this value is our best estimate for the scaling dimension of V . The curves show collapse within the error bars for $0.2 \leq t \leq 0.8$. We consider that the t values closer to the $x_3 = 0, L - 1$ boundaries are dominated by boundary effects and exclude them from the analysis.

To assign an error to our determination of Δ_V , we propose the following heuristic procedure.

⁷The way our measurement is organized, all points for the same L , and in particular the symmetric data points, are correlated with an unknown correlation. Thus once the measurement is finished, we cannot easily take advantage of this antisymmetry to reduce the errors by averaging over the symmetric datapoints. However, that the measured function does come out antisymmetric is a check of our procedure.

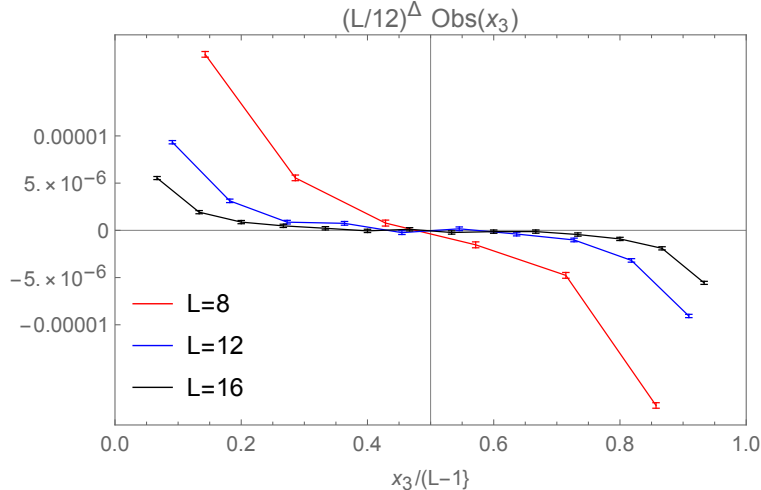


Fig. 2: In this plot $\Delta = 2$, testing (and ruling out) the virial current existence hypothesis.

We vary Δ around 6 and see when the curves clearly deviate from the collapsing behavior in the interval $0.2 \leq t \leq 0.8$, judging by the eye. One way to quickly perform this analysis is to use the `Manipulate` function of `Mathematica`. This way we arrive at our confidence interval $\Delta_V = 6 \pm 1$. See Fig. 4 for what the collapse plots look like at the extreme ends of the confidence interval.⁸ While the “judging by the eye” procedure may seem subjective and ad hoc, we don’t believe a much better statistical procedure can be advocated given our limited amount of data.

We have cross-checked our determination of Δ_V by focussing on the three points $x_3 = 2$ ($L = 8$), $x_3 = 3$ ($L = 12$) and $x_3 = 4$ ($L = 16$), which correspond to three close values of $t = x_3/(L - 1)$. Neglecting the difference in t , the values of the observable at these three points should scale as $const./L^{\Delta_V}$. That this is indeed roughly the case can be seen in the log-log plot in figure 5. Performing the fit using these three points and their mirror images under $t \rightarrow 1 - t$, we get the same answer $\Delta_V = 6 \pm 1$.

4. Conclusions

One goal of this paper was to emphasize that there is a simple and robust way to check the conformal invariance of any critical lattice model, which requires the measurement of the lowest non-derivative vector operator V which is a singlet under all global symmetries. This operator can play the role of the virial current, and potentially cause scale without conformal invariance, but only if its dimension is exactly $d - 1$.

⁸If we omit the $L = 8$ datapoints from our analysis (e.g. if one is worried that these points are still significantly affected by the subleading ... corrections in (2.4)), then we get $\Delta_V = 5.5 \pm 1.5$ using the same procedure. We quote this number only for comparison, as we do not feel that completely discarding the $L = 8$ points is justified.

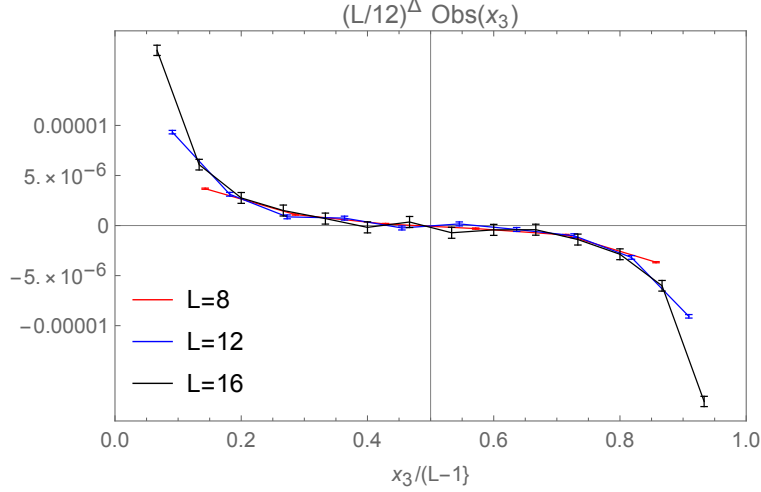


Fig. 3: In this plot $\Delta = 6$, which is our central value for Δ_V .

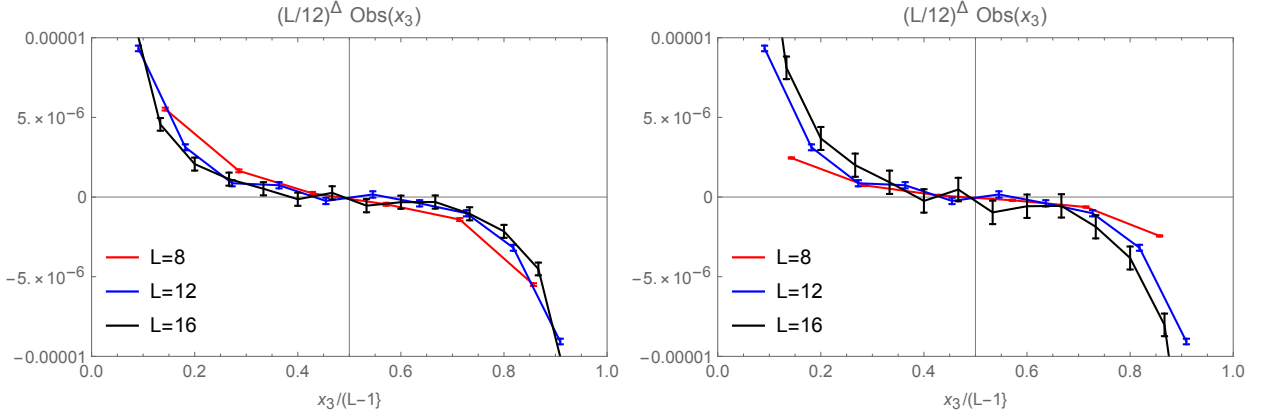


Fig. 4: Determining a confidence interval for Δ_V . Left: $\Delta = 5$. Right: $\Delta = 7$.

In this paper we concretely demonstrated this strategy by determining the dimension of V in the critical 3d Ising model: $\Delta_V = 6 \pm 1$. While the error bars are significant, the virial current value $\Delta_V = 2$ is soundly ruled out. This confirms that the 3d Ising model is conformally invariant.

Since the dimension of V is so large, to carry out our measurement we had to introduce several tricks increasing the efficiency of Monte Carlo simulations. In particular, we had to consider an integrated lattice operator to decouple uninteresting total derivative terms, and to optimize boundary conditions to maximize the (integrated) 1pt function of V , which was our Monte Carlo target. Further boundary condition optimization is likely possible (see appendix D) and will allow to reduce the error on Δ_V in future studies.

In this paper we have not carried out any correction-to-scaling analysis. It would be interesting to repeat the simulation in the Blume-Capel model which is in the same universality class as the Ising model but has a free parameter allowing to drastically reduce corrections to scaling [12].

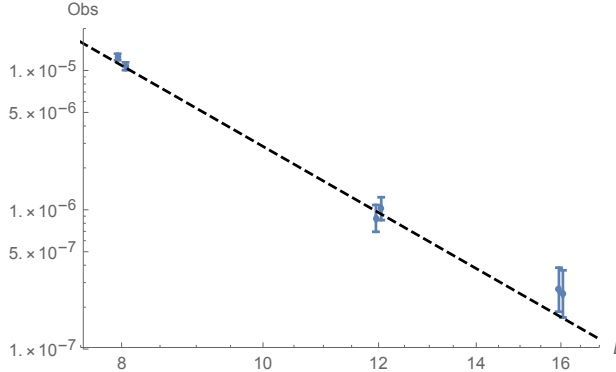


Fig. 5: Observable for $x_3 = 2$ ($L = 8$), $x_3 = 3$ ($L = 12$) and $x_3 = 4$ ($L = 16$) and for the three mirror points (with a minus sign). The dashed line is the best fit c/L^{Δ_V} which gives $\Delta_V = 6.03$ as the central value.

It would be also interesting to determine the dimension of V for the $O(N)$ and other models.

Finally, we would like to comment on the determination of Δ_V using the conformal bootstrap. The numerical conformal bootstrap has determined scaling dimensions of about 100 operators of the critical 3d Ising model [2]. The operators which have been determined appear in the operator product expansions (OPEs) of $\sigma \times \sigma$, $\varepsilon \times \varepsilon$ and $\sigma \times \varepsilon$, where σ and ε are the lowest dimension \mathbb{Z}_2 -odd and \mathbb{Z}_2 -even scalars. The OPEs $\sigma \times \sigma$ and $\varepsilon \times \varepsilon$, being OPEs of identical scalars, contain only operators of even spin. The OPE $\sigma \times \varepsilon$ contain only \mathbb{Z}_2 -odd operators. The operator V , being a \mathbb{Z}_2 -even vector, does not appear in these OPEs, and therefore it has not been so far probed by the conformal bootstrap. In the future, the OPEs $\sigma \times \sigma'$ and $\varepsilon \times \varepsilon'$, where σ' and ε' are the subleading \mathbb{Z}_2 -odd and \mathbb{Z}_2 -even scalars, will hopefully be included in the bootstrap analysis. These OPEs contain V and can be used to determine its dimension.

Of course, determination of Δ_V using the conformal bootstrap already presupposes that the model is conformally invariant. This has to be distinguished from the determination carried out in our paper, which was valid independently of conformal invariance, and so allowed us to test this property.

Acknowledgements

We would like to thank João Penedones for collaboration at the initial stages of this project, Leonardo Giusti and Agostino Patella for the useful discussions, and Matthijs Hogervorst and Agostino Patella for comments and suggestions for the draft. PY is grateful to the CERN Theoretical Physics Department for hospitality. SR and PY were supported by the National Centre of Competence in Research SwissMAP funded by the Swiss National Science Foundation. SR is supported by the Simons Foundation grant 488655 (Non-perturbative bootstrap), and by Mitsubishi

Heavy Industries as an ENS-MHI Chair holder. Calculations of this paper were performed at the CERN Theory cluster. We are grateful to the authors of ALPS [15] whose library was very useful for setting up preliminary simulations.

A. Dimension of V in the ϵ expansion

To be precise, in $d = 4$ there are two $\Delta = 7$ operators with the quantum numbers of V , which will mix:

$$O_1 = \phi \partial_\mu \phi (\partial \phi)^2, \quad O_2 = \phi^2 (\partial_\mu \partial_\nu \phi) \partial_\nu \phi.$$

To compute the anomalous dimension at the Wilson-Fisher fixed point, we have to compute the OPE with the perturbing operator ϕ^4 and extract the logarithmic divergence [16]. The relevant OPE coefficients integrated over the angular directions are:

$$O_1 \times \phi^4 = 60 O_1 + 8 O_2, \quad O_2 \times \phi^4 = 12 O_1 + 64 O_2.$$

This is in the same normalization in which $\phi^4 \times \phi^4 = 72 \phi^4$. The two linear combinations getting well-defined anomalous dimensions are:

$$(O_1 + O_2) \times \phi^4 = 72(O_1 + O_2), \quad (3O_1 - 2O_2) \times \phi^4 = 52(3O_1 - 2O_2).$$

The first linear combination is a descendant field, being the derivative of $\phi^2(\partial\phi)^2$. The other linear combination is the V . Its anomalous dimension is $52(\epsilon/36)$, leading to the total IR dimension (1.4).

B. Comment on Ref. [10]

The argument given in section VI of [10], that $\Delta_V > 2$ in the critical 3d Ising model, appears to us incorrect. The key step of their argument claims to show that the 2pt function of any \mathbb{Z}_2 -even vector lattice operator is bounded from above, at large distances, by the 2pt function of $\partial_\mu \varepsilon$, the derivative of the energy field ε . Since the energy field is rigorously known to have IR dimension > 1 , one gets $\Delta_V > 1 + \Delta_\varepsilon > 2$.

We disagree with the justification of precisely the key step, given in the paragraph containing their Eq. (24) (starting from the words “we assume below that this scaling limit does exist in the following precise sense”) and the paragraph containing their Eqs. (40), (41). Ref. [10] works in the latticized ϕ^4 Euclidean quantum field theory in $d = 3$ dimensions. They consider classes of lattice operators which would agree if one assumes that fields vary smoothly on the lattice scale (we will call it “naive continuum limit”). The essential operators have the form

$$\phi(x + e_1)\phi(x + e_2)\phi(x + e_3)\nabla_\mu \phi(x), \tag{B.1}$$

where ∇_μ is the lattice derivative, and $e_i = O(a)$ are some constant lattice vectors. In the naive continuum limit when e_i is dropped, all such operators are proportional to $\nabla_\mu(\phi^4)$. Ref. [10] claims that it is the naive continuum limit which determines the long-distance asymptotics. Therefore all operators (B.1) have the same asymptotic connected 2pt function behavior as the operator $\nabla_\mu(\phi^4)$ (up to some constant rescaling which may depend on e_i). Given that the lattice operator ϕ^4 interpolates the critical point energy operator ϵ , this allows them to conclude the argument.

Ref. [10] formalizes the procedure of dropping the vectors e_i through the property of “scaling limit”, introduced in their Eq. (24). They claim that it is “of course, satisfied to all orders of perturbation theory in any renormalizable theory”. Unfortunately, no reference is given to a proof or even any prior discussion of their Eq. (24) in the literature. This omission is in stark contrast with the other parts of their section VI, where they are trying to be exceedingly rigorous (for example they use the rigorous Lebowitz inequalities from the mathematical physics literature on lattice models). As a matter of fact, we believe that Eq. (24) in [10] is generally wrong.⁹

Here is a simple example of how modifying an operator at the lattice scale can change the long-distance asymptotics. Consider in the theory of a *complex* scalar field ϕ the lattice operator

$$\phi(x + e_1)\phi(x + e_2)\phi^*(x + e_3)\nabla_\mu\phi^*(x) + \phi^*(x + e_4)\phi^*(x + e_5)\phi(x + e_6)\nabla_\mu\phi(x). \quad (\text{B.2})$$

In the naive continuum limit, no matter what e_i are, this operator is proportional to $\nabla_\mu[(\phi\phi^*)^2]$. If the argument of Ref. [10] were universally valid, it would allow to conclude that any nonderivative vector operator in the $O(2)$ model in 3d has dimension > 2 . But we know that this model contains the conserved current $J_\mu = \phi\partial_\mu\phi^* - \phi^*\partial_\mu\phi$ which has dimension exactly 2. For generic unequal e_i , this current operator will couple to the above lattice operator and will dominate the long-distance behavior of its 2pt function.

Since this example shows that Eq. (24) in [10] is generally wrong, the argument that $\Delta_V > 1 + \Delta_\epsilon$ based on this equation cannot be accepted as a proof.

To avoid any possible misunderstanding, the following concluding comment may be useful. Although Eq. (24) in [10] is generally false, it may of course turn out to be true in some specific situations under some extra assumptions. For example, if it is known from some other source that $\Delta_V > 1 + \Delta_\epsilon$ (for example once Δ_V is measured via Monte Carlo simulations, as we did in this paper), then it can indeed be concluded that the leading behavior of the particular operators (B.1) is the same as for $\nabla_\mu(\phi^4)$, justifying this very particular case of Eq. (24) in [10]. Of course such a justification would not save their argument, since their very purpose was to try to use Eq. (24) to get information about Δ_V , not the other way around.

⁹One of us (SR) made extensive inquiries about this problem with the authors of Ref. [10] back in 2015, obtaining no satisfactory clarification.

C. Possible boundary conditions

One can imagine modifying our setup described in the main text, by changing the boundary conditions at $x_3 = 0, L - 1$. The purpose would be to find boundary conditions which lead to an even larger $f(t)$ and thus improve the signal-to-noise ratio. It makes sense to keep translation invariance in the x_2 direction, so that $\langle I(x_2, x_3) \rangle$ is x_2 independent and can be averaged in this direction.

As discussed in the main text, we have to break the x_1 flip symmetry. One way to do this is to choose different boundary conditions for different parts of the $x_3 = 0, L - 1$ boundaries, depending on x_1 .

In addition to the free and fixed boundary conditions (b.c.) described in the main text, there are two other imaginable types of b.c. worth discussing.

C.1. Gluing b.c.

The gluing b.c. changes topology of our manifold, by gluing one part of the boundary to another. For example, one can imagine gluing the gray parts of the $x_3 = 0, L - 1$ boundaries in Fig. 1, instead of imposing the fixed b.c. there. In practice, gluing is achieved by identifying points pairwise or, equivalently in the large L limit, by creating links joining the points being glued. In the just mentioned example, we would be identifying points

$$(x_1, x_2, x_3 = L - 1) \quad \text{with} \quad (x_1 + L/4, x_2, x_3 = 0) \quad (0 \leq x_1 < L/2, 0 \leq x_2 < L)$$

Gluing does not have to preserve order, for example we could have instead chosen to glue the gray parts of the boundaries while simultaneously flipping the x_1 coordinate. Such a reversed gluing would be a different boundary condition.

One can even glue parts of the same boundary, e.g. the lower and upper white parts of the $x_3 = 0$ boundary in Fig. 1 (again, in the direct or the reversed x_1 order).

C.2. Changing the strength of boundary interactions

We may change the strength of interaction among spins belonging to some part of the boundary to $\beta_{\text{bdry}} \neq \beta_c$. Two particularly interesting values of β_{bdry} are as follows.

$\beta_{\text{bdry}} = \beta_{\text{sp}} \approx 0.33302$. This fixes β_{bdry} to the value corresponding to the “special” boundary phase transition. Recall that the special transition separates the “ordinary” boundary behavior for which the boundary remains disordered at the critical temperature, from the “extraordinary” one when the boundary is ordered at the critical temperature. The ordinary (extraordinary) behavior is realized at $\beta_{\text{bdry}} < \beta_{\text{sp}}$ ($\beta_{\text{bdry}} > \beta_{\text{sp}}$). The β_{sp} for the 3d Ising model given above was determined in [17]. Since the boundary points have fewer neighbors than the bulk points, $\beta_{\text{bdry}} = \beta_c$ belongs to the “ordinary” phase, and this explains why $\beta_{\text{sp}} > \beta_c$.

$\beta_{\text{bdry}} = \infty$. This enforces that all spins are equal along a part of the boundary, which is the maximally efficient way to enforce the “extraordinary” boundary behavior. Notice that unlike the fixed boundary condition, the spins can still fluctuate between ± 1 , but only all at once. This difference may seem minor, but it has the following practical consequence. The fixed b.c. can be used if the simulations are performed using the Metropolis algorithm, as in the main text. On the other hand, if the simulations are performed using cluster algorithms, it leads to lowering the acceptance rate since clusters which touch the boundary cannot be flipped. The $\beta_{\text{bdry}} = \infty$ boundary condition does not have this difficulty.

There are many imaginable combinations of the four boundary condition types which break symmetries of the lattice in a way which makes $f(t)$ nonzero. It is tedious to simulate one by one all possible combinations for the Ising model and see which one gives the largest $f(t)$. It would be nice to have a way to guess a good boundary condition. A heuristic method is described in the next appendix.

D. Heuristic optimization of boundary conditions

Consider the free massless scalar theory on the cubic lattice, described by the action:

$$H = \sum_{\langle xy \rangle} (\phi(x) - \phi(y))^2, \quad \phi(x) \in \mathbb{R}.$$

We consider in this theory a lattice operator V_{μ}^{lat} given by the same equation (2.1) with $\phi(x)$ instead of $s(x)$. We make a heuristic hypothesis that one can get an idea about the size of $\langle I \rangle$ in the critical Ising model by measuring the same quantity in the free scalar theory on the same cubic lattice. One motivation for this hypothesis is that in $d = 4$ the two theories are actually identical. We won’t attempt to justify this hypothesis any further. It’s amusing that empirically it seems to work. Once the b.c. is so heuristically guessed, the actual hard computation will be an honest Monte Carlo simulation in the 3d Ising.

To use the heuristic, we have to establish a correspondence between boundary conditions for the two models. This correspondence is as follows:

1. The free b.c. in the Ising corresponds to the Dirichlet b.c. for the free scalar. Indeed, the free b.c. in Ising leads to the “ordinary” boundary behavior, where the order parameter is effectively zero on the boundary [16].
2. The gluing b.c. in Ising clearly corresponds to the same gluing for the free scalar.
3. $\beta_{\text{bdry}} = \infty$ for the Ising corresponds to imposing that $\phi(x)$ remains constant on this part of the boundary for the scalar.

4. $\beta_{\text{bdry}} = \beta_{\text{sp}}$ for the Ising corresponds to the Neumann (i.e. free) boundary condition for the scalar [16].
5. The fixed 3d Ising boundary condition can be modeled by adding a constant magnetic field (linear in $\phi(x)$ term) on the boundary, pushing the free scalar in the needed direction.

We won't give full details on how one actually performs the calculation for the free scalar. This calculation is inexpensive since one is computing a gaussian path integral. One constructs the lattice action, evaluates the Green's function, and finally evaluates the observable. The computation is done numerically and takes only a few seconds for a given boundary condition. The most expensive step is the Green's function evaluation which requires to invert an $L^3 \times L^3$ matrix.

After playing with the free scalar, we concluded that the boundary condition in Fig. 1 is particularly promising. Notice that since we have the same fixed b.c. on two parts of the boundary, and since we measure a \mathbb{Z}_2 -even observable, for the purpose of the heuristic computation we could replace the fixed boundary condition with $\beta_{\text{bdry}} = \infty$.

Before we discovered the heuristic optimization trick, we tried other boundary conditions in the 3d Ising, but they led to a smaller $f(t)$.

We could have just postulated the boundary condition in Fig. 1, but we prefer to play in the open. This is because we have not performed exhaustive optimization. Even better b.c. likely exist, and our heuristic may be helpful to search for them.

References

- [1] S. El-Showk, M. F. Paulos, D. Poland, S. Rychkov, D. Simmons-Duffin & A. Vichi, “*Solving the 3D Ising Model with the Conformal Bootstrap*”, Phys. Rev. **D86**, 025022 (2012), [arXiv:1203.6064](#). ♦ S. El-Showk, M. F. Paulos, D. Poland, S. Rychkov, D. Simmons-Duffin & A. Vichi, “*Solving the 3d Ising Model with the Conformal Bootstrap II. c-Minimization and Precise Critical Exponents*”, J. Stat. Phys. **157**, 869 (2014), [arXiv:1403.4545](#). ♦ F. Kos, D. Poland & D. Simmons-Duffin, “*Bootstrapping Mixed Correlators in the 3D Ising Model*”, JHEP **1411**, 109 (2014), [arXiv:1406.4858](#). ♦ D. Simmons-Duffin, “*A Semidefinite Program Solver for the Conformal Bootstrap*”, JHEP **1506**, 174 (2015), [arXiv:1502.02033](#). ♦ F. Kos, D. Poland, D. Simmons-Duffin & A. Vichi, “*Precision Islands in the Ising and $O(N)$ Models*”, JHEP **1608**, 036 (2016), [arXiv:1603.04436](#).
- [2] D. Simmons-Duffin, “*The Lightcone Bootstrap and the Spectrum of the 3d Ising CFT*”, JHEP **1703**, 086 (2017), [arXiv:1612.08471](#).
- [3] M. Billó, M. Caselle, D. Gaiotto, F. Gliozzi, M. Meineri & R. Pellegrini, “*Line defects in the 3d Ising model*”, JHEP **1307**, 055 (2013), [arXiv:1304.4110](#). ♦ C. Cosme, J. M. V. P. Lopes

- & J. Penedones, “*Conformal symmetry of the critical 3D Ising model inside a sphere*”, JHEP **1508**, 022 (2015), [arXiv:1503.02011](#).
- [4] G. Gori & A. Trombettoni, “*Conformal invariance in three dimensional percolation*”, J. Stat. Mech. **1507**, P07014 (2015), [arXiv:1504.07209](#).
- [5] J. Polchinski, “*Scale and Conformal Invariance in Quantum Field Theory*”, Nucl. Phys. **B303**, 226 (1988).
- [6] Y. Nakayama, “*Scale invariance vs conformal invariance*”, Phys. Rept. **569**, 1 (2015), [arXiv:1302.0884](#).
- [7] M. F. Paulos, S. Rychkov, B. C. van Rees & B. Zan, “*Conformal Invariance in the Long-Range Ising Model*”, Nucl. Phys. **B902**, 246 (2016), [arXiv:1509.00008](#).
- [8] V. Riva & J. L. Cardy, “*Scale and conformal invariance in field theory: A Physical counterexample*”, Phys. Lett. **B622**, 339 (2005), [hep-th/0504197](#).
- [9] S. El-Showk, Y. Nakayama & S. Rychkov, “*What Maxwell Theory in $D \neq 4$ teaches us about scale and conformal invariance*”, Nucl. Phys. **B848**, 578 (2011), [arXiv:1101.5385](#).
- [10] B. Delamotte, M. Tissier & N. Wschebor, “*Scale invariance implies conformal invariance for the three-dimensional Ising model*”, Phys. Rev. **E93**, 012144 (2016), [arXiv:1501.01776](#).
- [11] Y. Deng & H. W. J. Blöte, “*Simultaneous analysis of several models in the three-dimensional Ising universality class*”, Phys. Rev. E **68**, 036125 (2003).
- [12] M. Hasenbusch, “*Finite size scaling study of lattice models in the three-dimensional Ising universality class*”, Phys. Rev. B **82**, 174433 (2010), [arXiv:1004.4486](#).
- [13] L. Giusti & H. B. Meyer, “*Implications of Poincare symmetry for thermal field theories in finite-volume*”, JHEP **1301**, 140 (2013), [arXiv:1211.6669](#). ♦ L. Giusti & M. Pepe, “*Equation of state of the $SU(3)$ Yang-Mills theory: A precise determination from a moving frame*”, Phys. Lett. **B769**, 385 (2017), [arXiv:1612.00265](#).
- [14] U. Wolff, “*Collective Monte Carlo Updating for Spin Systems*”, Phys. Rev. Lett. **62**, 361 (1989).
- [15] A. Albuquerque, F. Alet, P. Corboz, P. Dayal, A. Feiguin, S. Fuchs, L. Gamper, E. Gull, S. Guertler, A. Honecker, R. Igarashi, M. Krner, A. Kozhevnikov, A. Läuchli, S. Manmana, M. Matsumoto, I. McCulloch, F. Michel, R. Noack, G. Pawłowski, L. Pollet, T. Pruschke, U. Schollwöck, S. Todo, S. Trebst, M. Troyer, P. Werner & S. Wessel, “*The ALPS project release 1.3: Open-source software for strongly correlated systems*”, Journal of Magnetism and Magnetic Materials **310**, 1187 (2007), Proceedings of the 17th International Conference on Magnetism. ♦ B. Bauer, L. D. Carr, H. G. Evertz, A. Feiguin, J. Freire, S. Fuchs, L. Gamper, J. Gukelberger, E. Gull, S. Guertler, A. Hehn, R. Igarashi, S. V. Isakov, D. Koop,

P. N. Ma, P. Mates, H. Matsuo, O. Parcollet, G. Pawłowski, J. D. Picon, L. Pollet, E. Santos, V. W. Scarola, U. Schollwöck, C. Silva, B. Surer, S. Todo, S. Trebst, M. Troyer, M. L. Wall, P. Werner & S. Wessel, “*The ALPS project release 2.0: open source software for strongly correlated systems*”, Journal of Statistical Mechanics: Theory and Experiment **2011**, P05001 (2011).

[16] J. L. Cardy, “*Scaling and renormalization in statistical physics*”, Cambridge, UK: Univ. Pr. (1996), 238 p..

[17] M. Hasenbusch, “*Monte Carlo study of surface critical phenomena: The special point*”, Phys. Rev. B **84**, 134405 (2011), [arXiv:1108.2425](https://arxiv.org/abs/1108.2425).